

Direct quark transition potential for $\Lambda N \rightarrow NN$ decayTakashi Inoue*, Sachiko Takeuchi^(a) and Makoto Oka*Department of Physics, Tokyo Institute of Technology**Meguro, Tokyo 152, Japan*

and

^(a)*Department of Public Health and Environmental Science**Tokyo Medical and Dental University**Yushima, Bunkyo, Tokyo, 113, Japan*

The weak $\Lambda N \rightarrow NN$ transition is studied in the valence quark model approach. The quark component of the two baryon system is described in the quark cluster model and the weak transition potential is calculated by evaluating the matrix elements of the $\Delta S = 1$ effective weak Hamiltonian. The transition potential is applied to the decay of hypernuclei and the results are compared with available experimental data. The results indicate that direct quark process is significant and qualitatively different when compared with those in conventional meson-exchange calculations. The direct quark mechanism predicts the violation of the $\Delta I = 1/2$ rule for this transition.

*e-mail: tinoue@th.phys.titech.ac.jp

1. Introduction

Non-leptonic weak decays of hyperons have been of interest for many years. Especially mesonic decays, such as $\Lambda \rightarrow N\pi$, are studied in order to reveal the properties of the low energy weak interactions among quarks. Experimental data for such decays indicate a strong $\Delta I = 1/2$ enhancement compared to $\Delta I = 3/2$ component. This $\Delta I = 1/2$ enhancement, known as the $\Delta I = 1/2$ rule, is not expected naively in the standard model of the weak interaction, and therefore its origin should be attributed for corrections to the weak vertex due to the strong interaction. Part of the strong corrections can be estimated by using the renormalization group improved perturbation theory of QCD[1,2,3,4], while contributions of the low-energy hadronic interactions are not quantitatively understood.

In order to study the corrections to the weak interaction due to the low-energy hadronic interaction, it may be useful to look into a new type of weak processes, such as $NN \rightarrow NN$, and $\Lambda N \rightarrow NN$, *i.e.*, the two-body weak scattering processes. It is known that the $\Lambda N \rightarrow NN$ transition plays a dominant role in the nonmesonic decays of hypernuclei, whose data have been accumulated in recent hypernuclear experiments. Therefore it seems timely to study the $\Lambda N \rightarrow NN$ weak transition from the standard theory point of view.

The purpose of this paper is to study the roles of quark structure in the two-body $\Lambda N \rightarrow NN$ weak transition, and to construct the induced transition potential [5,6,7,8]. Because the $\Lambda N \rightarrow NN$ decay has a large momentum transfer of approximately 420 MeV/c (assuming the relative momentum of the initial Λ and N is zero), the short distance dynamics of two baryons must be significant. We here propose that the $\Lambda N \rightarrow NN$ transition at short distance is described by a direct quark mechanism, where a contact four-quark interaction between the

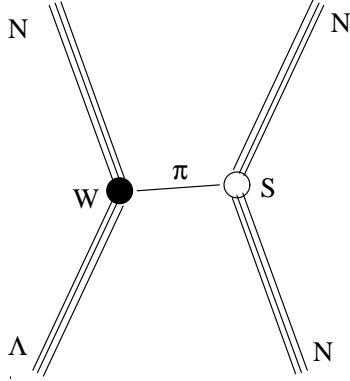


Figure 1: The diagram for the one pion exchange mechanism

constituent quarks of baryons causes the transition without exchanging mesons. The four-quark vertex is taken from the low energy effective weak Hamiltonian in the standard theory. It contains both the $\Delta I = 1/2$ and $\Delta I = 3/2$ components. We will see that no $\Delta I = 1/2$ enhancement is seen in the two-baryon process, $\Lambda N \rightarrow NN$, and thus the $\Delta I = 3/2$ component of the weak interaction may be observed.

We will compare the direct quark transition potential with the transition potentials based on the meson exchange mechanism (Fig. 1), such as π , K , ρ exchanges [9,10,11,12]. There the meson-baryon-baryon (such as $\pi - \Lambda - N$) weak vertex is determined phenomenologically so as to describe the free hyperon decays, and therefore satisfies the $\Delta I = 1/2$ rule automatically. Recent experimental data, however, have revealed some difficulties in the meson exchange picture. For instance, the predicted n - p ratio is much smaller than the experimental data for light hypernuclei.

This paper is organized as follows. In section 2, we present the effective weak Hamiltonian derived in the standard theory with perturbation in QCD. In section 3, the weak Hamiltonian is applied to the $\Lambda N \rightarrow NN$ transition and the direct quark induced transition potential $V(k, k')$

is calculated. In section 4, we present the explicit form of the transition potential given in the momentum space. In sections 5 and 6, the transition potential is applied to the decay of light hypernuclei and the results are compared with available experimental data. Discussions and conclusions are given in section 7.

2. Effective 4-quark weak interaction

The standard model describes hadronic weak interactions by exchanges of the weak gauge bosons between quarks. Because the gauge bosons are very heavy, low energy phenomena can effectively be represented by a Hamiltonian composed of four-quark vertices, which contain the QCD corrections on the pure weak vertex. Such an effective Hamiltonian has been studied by several authors[1,2,3,4]. It can be computed by evaluating the perturbative QCD corrections, using the operator product expansion and the renormalization group equation for the Wilson coefficients.

In the standard model, strangeness changing weak decay is described by the vertex

$$H_W(x) = \frac{g}{2\sqrt{2}} J_\mu^+(x) W_\mu^-(x) + H.c. , \quad (1)$$

where W_μ^\pm is the charged-W-boson field and J_μ^\pm is the hadronic charged weak current. Note that the standard theory contains no flavor changing neutral current. The effective Hamiltonian for $\Delta S = \pm 1$ nonleptonic processes is defined by

$$\langle | H_{eff}^{\Delta S=1} | \rangle = -\frac{i}{2} \int d^4x \langle | T H_W(x) H_W(0) | \rangle \quad (2)$$

where RHS is the weak transition matrix element between low-momentum hadron states composed of light quarks and differing in strangeness by one. We separate the mass-scale

dependent coefficients and the four-quark operators using the operator-product-expansion. At the mass scale $\mu = M_W$ the QCD running coupling constant α_s is so small that the coefficients can be expanded perturbatively in α_s . Paschos *et al.* [3] takes the following Hamiltonian at $\mu = M_W$,

$$H_{eff}^{\Delta S=1}\Big|_{\mu=M_W} = \frac{G_f}{\sqrt{2}} [\xi_u(\bar{s}_\alpha u_\alpha)_{V-A}(\bar{u}_\beta d_\beta)_{V-A} + \xi_c(\bar{s}_\alpha c_\alpha)_{V-A}(\bar{c}_\beta d_\beta)_{V-A}] + H_{peng}(\text{t-quark})(3)$$

where α and β stand for color indices of the quark field. The first term is a pure weak interaction at low-momentum transfer with $\xi_q = V_{qd}V_{qs}^*$ where matrix V is the Cabibbo-Kobayashi-Maskawa matrix. This term contains $\Delta I = 3/2$ component as well as $\Delta I = 1/2$ component. The second term, $H_{peng}(\text{t-quark})$, represents the first order QCD correction that is produced by a so-called penguin diagram with the top quark in the intermediate line. This term is needed because the top quark is heavier than the W-boson. Starting from eq.(3) at $\mu = M_W$ the effective Hamiltonian at low mass scale is computed with the help of the renormalization group technique. The one loop QCD corrections are taken into account. Operator mixing takes place and enhances the $\Delta I = 1/2$ component, while the $\Delta I = 3/2$ part is suppressed.

The perturbation theory, of course, cannot be extended down to the low energy region, where non-perturbative effects of QCD may modify the weak vertex as well. Here we employ the picture proposed by Bardeen *et al.*[13], *i.e.*, we assume that the perturbative correction is applied down to $\mu^2 \simeq \mu_0^2$, where $\alpha(\mu_0^2) = 1$ The effective four-quark Hamiltonians is calculated at μ_0^2 , and is applied to the quark model calculation (or any other low energy theory, such as the chiral effective theory).

We use the following Hamiltonian in the present calculation :

$$H_{eff}^{\Delta S=1}(\mu = \mu_0) = -\frac{G_f}{\sqrt{2}} \sum_{r=1, r \neq 4}^6 K_r O_r, \quad (4)$$

where

K_1	K_2	K_3	K_5	K_6
-0.284	0.009	0.026	0.004	-0.021

and

$$O_1 = (\bar{d}_\alpha s_\alpha)_{V-A} (\bar{u}_\beta u_\beta)_{V-A} - (\bar{u}_\alpha s_\alpha)_{V-A} (\bar{d}_\beta u_\beta)_{V-A} \quad (5)$$

$$O_2 = (\bar{d}_\alpha s_\alpha)_{V-A} (\bar{u}_\beta u_\beta)_{V-A} + (\bar{u}_\alpha s_\alpha)_{V-A} (\bar{d}_\beta u_\beta)_{V-A} \\ + 2(\bar{d}_\alpha s_\alpha)_{V-A} (\bar{d}_\beta d_\beta)_{V-A} + 2(\bar{d}_\alpha s_\alpha)_{V-A} (\bar{s}_\beta s_\beta)_{V-A} \quad (6)$$

$$O_3 = 2(\bar{d}_\alpha s_\alpha)_{V-A} (\bar{u}_\beta u_\beta)_{V-A} + 2(\bar{u}_\alpha s_\alpha)_{V-A} (\bar{d}_\beta u_\beta)_{V-A} \\ - (\bar{d}_\alpha s_\alpha)_{V-A} (\bar{d}_\beta d_\beta)_{V-A} - (\bar{d}_\alpha s_\alpha)_{V-A} (\bar{s}_\beta s_\beta)_{V-A} \quad (7)$$

$$O_5 = (\bar{d}_\alpha s_\alpha)_{V-A} (\bar{u}_\beta u_\beta + \bar{d}_\beta d_\beta + \bar{s}_\beta s_\beta)_{V+A} \quad (8)$$

$$O_6 = (\bar{d}_\alpha s_\beta)_{V-A} (\bar{u}_\beta u_\alpha + \bar{d}_\beta d_\alpha + \bar{s}_\beta s_\alpha)_{V+A}. \quad (9)$$

The values of the coefficients K_r are taken from ref.[3]. We choose the version with the flavor dependent Λ_{QCD} , $m_t = 200 \text{ GeV}/c^2$ and $\mu_0 = 0.24 \text{ GeV}$. The value of μ_0 is chosen so as to give $\alpha_s(\mu_0^2) = 1$ for $\Lambda_{QCD} = 0.1 \text{ GeV}$. Among the 4-quark operators above, O_3 contains a part which induces the $\Delta I = 3/2$ transition, while the others are purely $\Delta I = 1/2$. One sees that the O_1 component is enhanced, which is purely $\Delta I = 1/2$.

It is known that this $\Delta I = 1/2$ enhancement alone cannot explain the observed ratio of $\Delta I = 1/2$ and $\Delta I = 3/2$ for the non-leptonic decays of K , Λ and other strange hadrons.

Several studies have shown that various non-perturbative effects at low energy are crucial in understanding the large $\Delta I = 1/2$ enhancement[13,14,15].

3. Direct quark mechanism

The weak transition of two baryon systems can be described by a transition potential V . We evaluate V in the first order perturbation theory in the effective weak Hamiltonian $H_{eff}^{\Delta S=1}$ derived in the previous section,

$$V(k, k') \Big|_{L_f, S_f, J}^{L_i, S_i, J} = \langle NN(k', L_f, S_f, J) | H_{eff}^{\Delta S=1} | \Lambda N(k, L_i, S_i, J) \rangle. \quad (10)$$

We employ the quark cluster model for the quark component of the two baryon systems,

$$|BB'(L, S, J)\rangle = \mathcal{A}^6 |\phi(123)\phi(456)\chi(L, S, J)\rangle \quad (11)$$

where ϕ is the internal wave function of the baryon in the non-relativistic quark model and $\chi(\vec{R})$ is the wave function for the relative motion with \vec{R} , the relative coordinate of two baryons[16]. The operator \mathcal{A}^6 antisymmetrizes the six quarks. The transition potential eq.(10) describes the direct quark processes, in which all possible exchanges of quarks between two baryons are included (Fig. 2). These direct quark processes are independent from the meson exchange diagrams in our formulation because the non-relativistic formalism does not allow a pair of quark and antiquark in the intermediate state. Therefore the full transition should be given by a superposition of the direct quark and the meson exchange processes.

In evaluating the transition potential we make the non-relativistic reduction of $H_{eff}^{\Delta S=1}$ *i.e.* the Breit-Fermi expansion to first order in p/m . The result is given in terms of a set of non-relativistic operators listed in Table 1. The vectors \vec{q}_{ij} and \vec{P}_i are defined by

$$\vec{q}_{ij} = \vec{p}'_i - \vec{p}_i = \vec{p}'_j - \vec{p}_j \quad \vec{P}_i = \frac{\vec{p}_i + \vec{p}'_i}{2} \quad (12)$$

Table 1: The set of transition operators

$$\begin{aligned}
A1_{ij} &= [(d^\dagger s)_i (u^\dagger u)_j + (u^\dagger u)_i (d^\dagger s)_j] \otimes 1 \otimes 1 \\
A2_{ij} &= + \otimes (\vec{\sigma}_i \cdot \vec{\sigma}_j) \otimes 1 \\
A3_{ij} &= + \otimes (\vec{\sigma}_i - \vec{\sigma}_j) \otimes (\vec{q}_{ij}) \\
A4_{ij} &= + \otimes \otimes (\vec{P}_i - \vec{P}_j) \\
A5_{ij} &= - \otimes \otimes (\vec{P}_i + \vec{P}_j) \\
A6_{ij} &= + \otimes i (\vec{\sigma}_i \times \vec{\sigma}_j) \otimes (\vec{q}_{ij}) \\
A7_{ij} &= + \otimes \otimes (\vec{P}_i - \vec{P}_j) \\
A8_{ij} &= - \otimes \otimes (\vec{P}_i + \vec{P}_j) \\
A9_{ij} &= - \otimes (\vec{\sigma}_i + \vec{\sigma}_j) \otimes (\vec{q}_{ij}) \\
A10_{ij} &= - \otimes \otimes (\vec{P}_i - \vec{P}_j) \\
A11_{ij} &= + \otimes \otimes (\vec{P}_i + \vec{P}_j) \\
\\
B1_{ij} &= [(d^\dagger s)_i (d^\dagger d)_j + (d^\dagger d)_i (d^\dagger s)_j] \otimes 1 \otimes 1 \\
&\dots \\
B11_{ij} &= + \otimes (\vec{\sigma}_i + \vec{\sigma}_j) \otimes (\vec{P}_i + \vec{P}_j) \\
\\
C1_{ij} &= [(u^\dagger s)_i (d^\dagger u)_j + (d^\dagger u)_i (u^\dagger s)_j] \otimes 1 \otimes 1 \\
&\dots \\
C11_{ij} &= + \otimes (\vec{\sigma}_i + \vec{\sigma}_j) \otimes (\vec{P}_i + \vec{P}_j) .
\end{aligned}$$

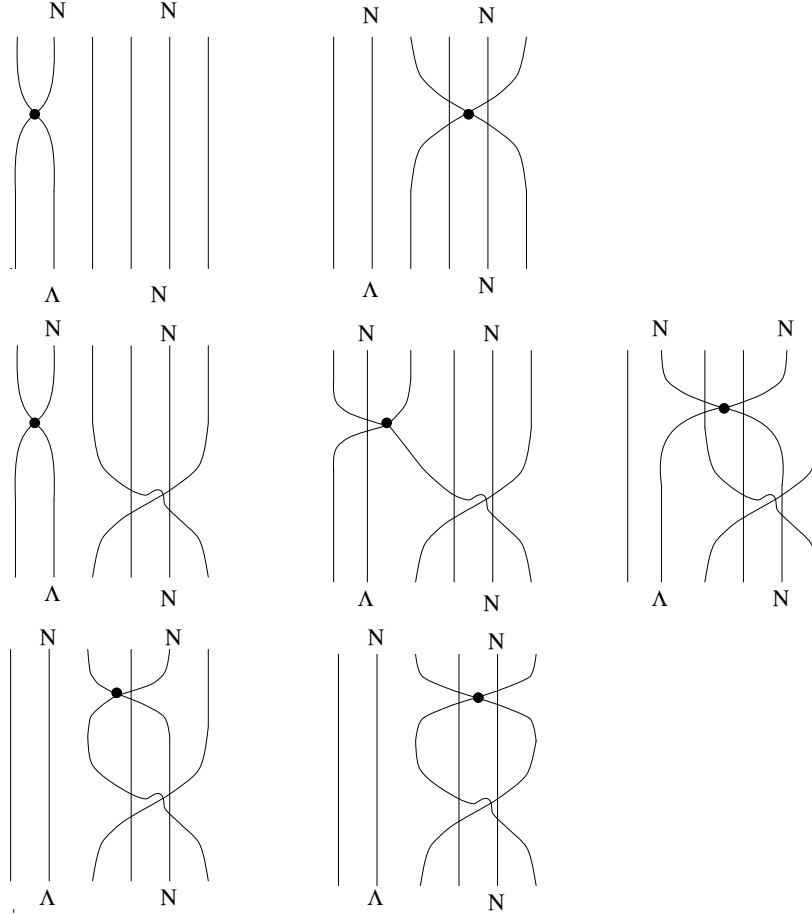


Figure 2: The diagrams for the direct quark mechanism

where \vec{p}_i denotes the momentum of the i -th quark. In Table 1, the color operator is suppressed, that is unity. Among those operators, the operators $A1, A2, B1, B2, C1$ and $C2$ are parity conserving, while the others are of first order in p/m and parity violating. These operators are symmetric in subscripts i and j . Appendix A gives the explicit form of $H_{eff}^{\Delta S=1}$ in terms of $\sum_{i<j} A1_{ij} \sim \sum_{i<j} C11_{ij}$. Because we truncate the expansion at p/m , the change of the orbital angular momentum, ΔL , is restricted to 0 or ± 1 , namely no tensor transition is allowed. In the present study, we restrict our initial state to $L = 0$ and 1. Table 2 shows 24 possible combinations of L, S, J , and I for the initial and final states. Note that the transition between 1P_1 and 3P_1 vanishes because the spin change operator should change the parity as well.

Table 2: Possible initial and final quantum numbers for transitions with initial $L = 0$ or 1

Ch	isospin	spin orbital	Type	W
1	$p\Lambda \rightarrow pn$	${}^1S_0 \rightarrow {}^1S_0$	1	1
2		$\rightarrow {}^3P_0$	2	$-\sqrt{3}$
3		${}^3S_1 \rightarrow {}^3S_1$	3	1
4		$\rightarrow {}^1P_1$	4	1
5		$\rightarrow {}^3P_1$	5	$-\sqrt{2}$
6		${}^1P_1 \rightarrow {}^3S_1$	F	1
7		$\rightarrow {}^1P_1$	G	1
8		$\rightarrow {}^3D_1$	F	$-\sqrt{\frac{5}{2}}$
9		${}^3P_0 \rightarrow {}^1S_0$	B	$-\sqrt{3}$
10		$\rightarrow {}^3P_0$	A	1
11		${}^3P_1 \rightarrow {}^3S_1$	C	$-\sqrt{2}$
12		$\rightarrow {}^3P_1$	A	1
13		$\rightarrow {}^3D_1$	C	$-\frac{\sqrt{5}}{2}$
14		${}^3P_2 \rightarrow {}^3P_2$	A	1
15		$\rightarrow {}^1D_2$	B	$\sqrt{\frac{3}{2}}$
16		$\rightarrow {}^3D_2$	C	$-\frac{3}{2}$
17	$n\Lambda \rightarrow nn$	${}^1S_0 \rightarrow {}^1S_0$	6	1
18		$\rightarrow {}^3P_0$	7	$-\sqrt{3}$
19		${}^3S_1 \rightarrow {}^3P_1$	8	$-\sqrt{2}$
20		${}^3P_0 \rightarrow {}^1S_0$	I	$-\sqrt{3}$
21		$\rightarrow {}^3P_0$	H	1
22		${}^3P_1 \rightarrow {}^3P_1$	H	1
23		${}^3P_2 \rightarrow {}^3P_2$	H	1
24		$\rightarrow {}^1D_2$	I	$-\sqrt{\frac{3}{2}}$

Matrix elements of $\sum_{i<j}^6 A1_{ij} \sim \sum_{i<j}^6 C11$ are calculated for the quark cluster model wave function. Under the condition that $|\phi\phi\chi\rangle$ is totally antisymmetric for the exchange $\{1,2,3\} \leftrightarrow \{4,5,6\}$, the matrix element, for instance

$$\langle B_3 B_4 | \sum_{i<j}^6 A1_{ij} | B_1 B_2 \rangle, \quad (13)$$

is equal to

$$\begin{aligned} & \frac{6}{N} \langle \phi\phi\chi | A1_{12} | \phi\phi\chi \rangle + \frac{9}{N} \langle \phi\phi\chi | A1_{36} | \phi\phi\chi \rangle \\ & - \frac{18}{N} \langle \phi\phi\chi | A1_{12} P_{36} | \phi\phi\chi \rangle - \frac{36}{N} \langle \phi\phi\chi | A1_{13} P_{36} | \phi\phi\chi \rangle \\ & - \frac{36}{N} \langle \phi\phi\chi | A1_{25} P_{36} | \phi\phi\chi \rangle - \frac{36}{N} \langle \phi\phi\chi | A1_{35} P_{36} | \phi\phi\chi \rangle \\ & - \frac{9}{N} \langle \phi\phi\chi | A1_{36} P_{36} | \phi\phi\chi \rangle \end{aligned} \quad (14)$$

where P_{36} represents the permutation operator, $3 \leftrightarrow 6$. Fig. 2 shows the diagrams corresponding to each term of eq.(14). Because each baryon wave function is totally antisymmetrized, \mathcal{A}^6 of the initial and final state can be replaced by a single P_{36} operated to the initial state. N is the normalization factor, which depends on the channel but is nearly equal to 1 in general. We factorize each matrix element in eq.(14) into the flavor-spin, orbital and color parts as

$$\begin{aligned} & \langle \phi\phi\chi(k', L_f, S_f, J) | A1_{ij}(P_{36}) | \phi\phi\chi(k, L_i, S_i, J) \rangle \\ & = \langle \phi\phi\chi^{\text{flavor-spin}} | A1_{ij}^{\text{flavor-spin}}(P_{36}^{\text{flavor-spin}}) | \phi\phi\chi^{\text{flavor-spin}} \rangle \\ & \quad \times \langle \phi\phi\chi^{\text{orbital}} | A1_{ij}^{\text{orbital}}(P_{36}^{\text{orbital}}) | \phi\phi\chi^{\text{orbital}} \rangle \\ & \quad \times \langle \phi\phi\chi^{\text{color}} | 1(P_{36}^{\text{color}}) | \phi\phi\chi^{\text{color}} \rangle \times W . \end{aligned} \quad (15)$$

W is an algebraic factor required when we factorize the spin and orbital matrix elements. It

is defined by

$$W = (-)^\lambda \sqrt{2\lambda+1} \sqrt{2J+1} \begin{Bmatrix} L_i & S_i & J \\ \lambda^o & \lambda^s & 0 \\ L_f & S_f & J \end{Bmatrix} \left\{ \frac{\sqrt{2L_f+1}}{(L_i, \lambda^o, L_z, 0 | L_f, L_z)} \frac{\sqrt{2S_f+1}}{(S_i, \lambda^s, S_z, 0 | S_f, S_z)} \right. \quad (16)$$

where λ^o and λ^s are the ranks of the orbital and spin operators respectively, and $\lambda = \lambda^o = \lambda^s$.

In Table 2, we label the combinations of the initial and the final spin-flavor part of $|\phi\phi\chi\rangle$ by ‘‘Type’’. They are listed in Table 14 in Appendix B. In evaluating the flavor-spin matrix element, we use the $SU(6)$ flavor-spin wave function for the nucleon and Λ .

Appendix C is devoted to evaluation of the orbital matrix elements

$$\langle \phi\phi\chi^{\text{orbital}}(k', L_f) | O_{ij}^{\text{orbital}}(P_{36}^{\text{orbital}}) | \phi\phi\chi^{\text{orbital}}(k, L_i) \rangle \quad (17)$$

where O_{ij}^{orbital} is one of the following operators,

$$1_{ij} \quad \times \delta(\vec{p}'_i + \vec{p}'_j - \vec{p}_i - \vec{p}_j) \quad (18)$$

$$\vec{q}_{ij} \quad \times \delta(\vec{p}'_i + \vec{p}'_j - \vec{p}_i - \vec{p}_j) \quad (19)$$

$$(\vec{P}_i - \vec{P}_j) \times \delta(\vec{p}'_i + \vec{p}'_j - \vec{p}_i - \vec{p}_j) \quad (20)$$

$$(\vec{P}_i + \vec{P}_j) \times \delta(\vec{p}'_i + \vec{p}'_j - \vec{p}_i - \vec{p}_j) . \quad (21)$$

Color matrix elements are given by

$$\langle \text{color-singlet} | 1 | \text{color-singlet} \rangle = 1, \quad (22)$$

$$\langle \text{color-singlet} | 1 P_{36}^{\text{color}} | \text{color-singlet} \rangle = 1/3. \quad (23)$$

4. Induced transition potential

The obtained $\Lambda N \rightarrow NN$ transition potential is written in the following form.

$$V(k, k') \Big|_{\substack{L_i, S_i, J \\ L_f, S_f, J}} = -\frac{G_F}{\sqrt{2}} \sum_{i=1}^7 \{V_i^f f(k, k')_i + V_i^g g(k, k')_i + V_i^h h(k, k')_i\} \times W \quad (24)$$

The coefficients, V^f , V^g and V^h and the functions, f , g and h are given in Tables 3 ~ 11. The numbers are normalized in the unit of $1/660 \times \sqrt{6}/1296$ for Type 1, 2, 3, 4, 5, A, B, C and F and in the unit of $1/660 \times \sqrt{3}/648$ for Type 6, 7, 8, H and I. In Tables 6 ~ 8, $\delta(L_i, L_f)$, $I(L_i, L_f)$, $\exp[ij]$ and $F(L, X)$ are defined by

$$\delta(L_i, L_f) = \delta_{L_i L_f} \quad (25)$$

$$I(L_i, L_f) = \int Y_{L_f}^{0*}(\Omega) \cos \theta Y_{L_i}^0(\Omega) d\Omega \quad (26)$$

$$\exp[12] = \frac{3\sqrt{6}}{4} \exp \left[-b^2 \frac{5}{12} (k^2 + k'^2) \right] \quad (27)$$

$$\exp[13] = \frac{24\sqrt{33}}{121} \exp \left[-b^2 \frac{1}{33} (7k^2 + 13k'^2) \right] \quad (28)$$

$$\exp[25] = \frac{3\sqrt{3}}{8} \exp \left[-b^2 \frac{1}{6} (k^2 + k'^2) \right] \quad (29)$$

$$\exp[35] = \frac{24\sqrt{33}}{121} \exp \left[-b^2 \frac{1}{33} (13k^2 + 7k'^2) \right] \quad (30)$$

$$\exp[36] = \exp \left[-b^2 \frac{1}{3} (k^2 + k'^2) \right] \quad (31)$$

$$F(0, X) = 4\pi \frac{\sinh(Xb^2kk')}{Xb^2kk'} \quad (32)$$

$$F(1, X) = -4\pi \left(\frac{\sinh(Xb^2kk')}{X^2b^4k^2k'^2} - \frac{\cosh(Xb^2kk')}{Xb^2kk'} \right) \quad (33)$$

The transition potential depends on three quark model parameters that are m , the constituent u, d quark mass, m_s , the strange quark mass and the Gaussian parameter b . The ratio m_s/m is chosen as 5/3 in the calculation of V^f , V^g and V^h . We use $m = 313$ MeV and $b = 0.5$ fm in the following section.

In order to study the contribution of $\Delta I = 3/2$ component of the $H_{eff}^{\Delta S=1}$, we also calculate the transition potential without the $\Delta I = 3/2$ component. Table 9 ~ Table 11 give the coefficients when we omit the $\Delta I = 3/2$ component.

Table 3: The coefficients V^f for the full Hamiltonian.

Ty.	V_1^f	V_2^f	V_3^f	V_4^f	V_5^f	V_6^f	V_7^f
1	-77588.4	29011.5	-787.2	6117.8	-10195.3	39068.5	-34345.4
3	-77588.4	29011.5	-787.2	303.9	-10195.3	4185.1	538.0
G	-77588.4	-79950.0	-163442.3	-79950.0	-50544.8	-162261.5	-162261.5
A	-77588.4	-44941.4	-34614.9	-13581.0	-22070.8	-13756.8	-12855.1
6	-77588.4	29011.5	-787.2	-67.5	-10195.3	1956.7	2766.4
H	-77588.4	-44941.4	-34614.9	-13581.0	-22070.8	-9633.2	-16978.7

Table 4: The coefficients V^g for the full Hamiltonian.

Ty.	V_1^g	V_2^g	V_3^g	V_4^g	V_5^g	V_6^g	V_7^g
2	-54.3	-297.1	15321.8	5760.4	-43.6	21392.9	-2476.8
4	-54.3	-84.6	69818.0	31586.4	1490.8	85572.9	84357.2
5	54.3	-122.8	-14966.7	-5465.2	-1767.2	-758.7	-2202.1
F	-54.3	184.6	314.9	-256.9	-6683.7	-57943.0	-52750.3
B	-54.3	214.6	166.3	-2266.7	-2239.4	-25126.8	12162.8
C	54.3	45.2	-142.0	53.9	-182.6	-1155.6	-261.3
7	-54.3	115.3	15321.8	5760.4	656.1	6823.1	12093.1
8	54.3	152.1	-14941.7	-5465.2	-1467.3	66.0	-3026.8
I	-54.3	-60.3	216.3	207.4	-2039.5	-3959.3	-9004.7

Table 5: The coefficients V^h for the full Hamiltonian.

Ty	V_1^h	V_2^h	V_3^h	V_4^h	V_5^h	V_6^h	V_7^h
2	-54.3	-297.1	-5116.0	-4602.0	-1294.7	-28090.4	17845.1
4	-54.3	-84.6	-23274.8	-759.8	-4683.2	-43698.3	-41266.8
5	54.3	-122.8	5007.7	-586.3	4817.9	-10152.2	-6002.8
F	-54.3	184.6	0.0	13521.8	19700.0	110914.1	106694.0
B	-54.3	214.6	69.6	1436.8	6307.2	21951.0	1772.9
C	54.3	45.2	95.6	295.2	439.2	3666.7	584.1
7	-54.3	115.3	-5116.0	552.4	-1469.7	-2249.6	-7995.7
8	54.3	152.1	4907.7	444.6	4742.9	-8502.8	-7652.2
I	-54.3	-60.3	-130.4	1436.8	6257.2	9305.5	14418.4

Table 6: The functions f_i

$$\begin{aligned}
 f(k, k')_1 &= \frac{6}{N} \delta(L_i, L_f) \sqrt{2\pi} \frac{1}{b^3} \frac{1}{k^2} \delta(k' - k) \\
 f(k, k')_2 &= -\frac{18}{N} \frac{1}{3} \delta(L_i, L_f) \exp[12] F\left(L_i, \frac{1}{2}\right) \\
 f(k, k')_3 &= -\frac{36}{N} \frac{1}{3} \delta(L_i, L_f) \exp[13] F\left(L_i, \frac{12}{33}\right) \\
 f(k, k')_4 &= -\frac{36}{N} \frac{1}{3} \delta(L_i, L_f) \exp[25] F(L_i, 0) \\
 f(k, k')_5 &= -\frac{36}{N} \frac{1}{3} \delta(L_i, L_f) \exp[35] F\left(L_i, \frac{12}{33}\right) \\
 f(k, k')_6 &= \frac{9}{N} \delta(L_i, L_f) \exp[36] F\left(L_i, \frac{2}{3}\right) \\
 f(k, k')_7 &= -\frac{9}{N} \frac{1}{3} \delta(L_i, L_f) \exp[36] F\left(L_i, \frac{2}{3}\right)
 \end{aligned}$$

Table 7: The functions g_i

$$\begin{aligned}
 g(k, k')_1 &= \frac{6}{N} \frac{1}{3} I(L_i, L_f) \frac{k}{m} \sqrt{2\pi} \frac{1}{b^3} \frac{1}{k^2} \delta(k' - k) \\
 g(k, k')_2 &= -\frac{18}{N} \frac{1}{3} I(L_i, L_f) \frac{k}{m} \exp[12] F\left(L_f, \frac{1}{2}\right) \\
 g(k, k')_3 &= -\frac{36}{N} \frac{1}{3} I(L_i, L_f) \frac{k}{m} \exp[13] F\left(L_f, \frac{12}{33}\right) \\
 g(k, k')_4 &= -\frac{36}{N} \frac{1}{3} I(L_i, L_f) \frac{k}{m} \exp[25] F(L_f, 0) \\
 g(k, k')_5 &= -\frac{36}{N} \frac{1}{3} I(L_i, L_f) \frac{k}{m} \exp[35] F\left(L_f, \frac{12}{33}\right) \\
 g(k, k')_6 &= \frac{9}{N} \frac{1}{3} I(L_i, L_f) \frac{k}{m} \exp[36] F\left(L_f, \frac{2}{3}\right) \\
 g(k, k')_7 &= -\frac{9}{N} \frac{1}{3} I(L_i, L_f) \frac{k}{m} \exp[36] F\left(L_f, \frac{2}{3}\right)
 \end{aligned}$$

Table 8: The functions h_i

$$\begin{aligned}
 h(k, k')_1 &= \frac{6}{N} \frac{1}{3} I(L_i, L_f) \frac{k'}{m} \sqrt{2\pi} \frac{1}{b^3} \frac{1}{k^2} \delta(k' - k) \\
 h(k, k')_2 &= -\frac{18}{N} \frac{1}{3} I(L_i, L_f) \frac{k'}{m} \exp[12] F\left(L_i, \frac{1}{2}\right) \\
 h(k, k')_3 &= -\frac{36}{N} \frac{1}{3} I(L_i, L_f) \frac{k'}{m} \exp[13] F\left(L_i, \frac{12}{33}\right) \\
 h(k, k')_4 &= -\frac{36}{N} \frac{1}{3} I(L_i, L_f) \frac{k'}{m} \exp[25] F(L_i, 0) \\
 h(k, k')_5 &= -\frac{36}{N} \frac{1}{3} I(L_i, L_f) \frac{k'}{m} \exp[35] F\left(L_i, \frac{12}{33}\right) \\
 h(k, k')_6 &= \frac{9}{N} \frac{1}{3} I(L_i, L_f) \frac{k'}{m} \exp[36] F\left(L_i, \frac{2}{3}\right) \\
 h(k, k')_7 &= -\frac{9}{N} \frac{1}{3} I(L_i, L_f) \frac{k'}{m} \exp[36] F\left(L_i, \frac{2}{3}\right)
 \end{aligned}$$

Table 9: The coefficients V^f for the $\Delta I = 1/2$ Hamiltonian.

Ty.	V_1^f	V_2^f	V_3^f	V_4^f	V_5^f	V_6^f	V_7^f
1	-77588.4	29011.5	-787.2	1994.3	-10195.3	14327.3	-9604.2
3	-77588.4	29011.5	-787.2	303.9	-10195.3	4185.1	538.0
G	-77588.4	-79950.0	-163442.3	-79950.0	-50544.8	-162261.5	-162261.5
A	-77588.4	-44941.4	-34614.9	-13581.0	-22070.8	-11007.7	-15604.2
6	-77588.4	29011.5	-787.2	1994.3	-10195.3	14327.3	-9604.2
H	-77588.4	-44941.4	-34614.9	-13581.0	-22070.8	-11007.7	-15604.2

Table 10: The coefficients V^g for the $\Delta I = 1/2$ Hamiltonian.

Ty.	V_1^g	V_2^g	V_3^g	V_4^g	V_5^g	V_6^g	V_7^g
2	-54.3	-22.2	15321.8	5760.4	422.9	11679.7	7236.5
4	-54.3	-84.6	69818.0	31586.4	1490.8	85572.9	84357.2
5	54.3	60.5	-14950.0	-5465.2	-1567.3	-208.9	-2751.9
F	-54.3	184.6	314.9	-256.9	-6683.7	-57943.0	-52750.3
B	-54.3	31.4	199.6	-617.3	-2106.2	-11015.1	-1948.9
C	54.3	45.2	-142.0	53.9	-182.6	-1155.6	-261.3
7	-54.3	-22.2	15321.8	5760.4	422.9	11679.7	7236.5
8	54.3	60.5	-14950.0	-5465.2	-1567.3	-208.9	-2751.9
I	-54.3	31.4	199.6	-617.3	-2106.2	-11015.1	-1948.9

Table 11: The coefficients V^h for the $\Delta I = 1/2$ Hamiltonian.

Ty.	V_1^h	V_2^h	V_3^h	V_4^h	V_5^h	V_6^h	V_7^h
2	-54.3	-22.2	-5116.0	-1165.8	-1411.3	-10863.2	617.9
4	-54.3	-84.6	-23274.8	-759.8	-4683.2	-43698.3	-41266.8
5	54.3	60.5	4941.0	101.0	4767.9	-9052.6	-7102.4
F	-54.3	184.6	0.0	13521.8	19700.0	110914.1	106694.0
B	-54.3	31.4	-63.7	1436.8	6273.8	13520.7	10203.2
C	54.3	45.2	95.6	295.2	439.2	3666.7	584.1
7	-54.3	-22.2	-5116.0	-1165.8	-1411.3	-10863.2	617.9
8	54.3	60.5	4941.0	101.0	4767.9	-9052.6	-7102.4
I	-54.3	31.4	-63.7	1436.8	6273.8	13520.7	10203.2

5. Application to light hypernuclear decays

We apply the transition potential to non-mesonic weak decays of light hypernuclei. We assume that the decay of Λ in nucleus is incoherent and that one can neglect final state interactions for two energetic outgoing nucleons and interference effects arising from the antisymmetrization of the final state. Then the decay rate of a light hypernucleus is given by a sum of two-body $\Lambda N \rightarrow NN$ transition rates. The decay of ${}^5_{\Lambda}\text{He}$, for instance, can be described in terms of the spin averaged two-body transition rates, $\Gamma_{\Lambda p \rightarrow pn}$ and $\Gamma_{\Lambda n \rightarrow nn}$, as

$$\Gamma({}^5_{\Lambda}\text{He}) = 2 \Gamma_{\Lambda p \rightarrow pn} + 2 \Gamma_{\Lambda n \rightarrow nn} . \quad (34)$$

where

$$\Gamma = \frac{1}{4} \sum_{\substack{S_i, \mu_i \\ S_f, \mu_f}} \int \frac{d^3 \vec{K}}{(2\pi)^3} 2\pi \delta(E.C.) \left| \int \frac{d^3 \vec{p}}{(2\pi)^3} \int \frac{d^3 \vec{q}}{(2\pi)^3} \psi_{fin}(\vec{q}; \vec{K}) V_{S_i, \mu_i}^{S_f, \mu_f}(\vec{p}, \vec{q}) \psi_{ini}(\vec{p}) \right|^2 . \quad (35)$$

Here $\psi_{ini}(\vec{p})$ and $\psi_{fin}(\vec{q}; \vec{K})$ are the initial and final two-body wave functions and $V(\vec{p}, \vec{q})$ is the transition potential. In the present study, we also neglect the binding energy of the initial state, and use the following energy conservation rule,

$$\delta(E.C.) = \frac{M_N}{2K} \delta(K - K^*) \quad (36)$$

where $K^* = 415.9$ MeV satisfies

$$M_\Lambda + M_N = 2 \frac{K^{*2}}{2M_N} + 2M_N . \quad (37)$$

Decomposing ψ into partial waves and performing the \vec{K} integration, one obtains

$$\Gamma = \frac{1}{(2\pi)^2} \frac{M_N K^*}{2} \frac{1}{4} \sum_{\substack{L_i, S_i, J, m \\ L_f, S_f, J, m}} \left| \int \frac{p^2 dp}{(2\pi)^3} \int \frac{q^2 dq}{(2\pi)^3} \psi_{L_f}^{fin}(q; K^*) V_{L_i, S_i, J}^{L_f, S_f, J}(p, q) \psi_{L_i}^{ini}(p) \right|^2, \quad (38)$$

where ψ_L is the radial part of the wave function and $V_{L_i, S_i, J}^{L_f, S_f, J}(p, q)$ is the partial wave decomposed transition potential. For the decay of S-shell hypernuclei, we neglect $L \neq 0$ components of the ground state wave function and thus only the transitions from the S wave initial states to the final plane wave are considered. They correspond to the channels, $1 \sim 5$ for $\Lambda p \rightarrow pn$, and $17 \sim 19$ for $\Lambda n \rightarrow nn$, in Table 2. We label the transition amplitudes by a through f as

$$\begin{array}{l} a_p \ a_n \\ b_p \ b_n \\ c_p \\ d_p \\ e_p \\ f_p \ f_n \end{array} \left| \begin{array}{l} {}^1S_0 \rightarrow {}^1S_0 \\ \phantom{{}^1S_0} \rightarrow {}^3P_0 \\ {}^3S_1 \rightarrow {}^3S_1 \\ \phantom{{}^3S_1} \rightarrow {}^3D_1 \\ \phantom{{}^3S_1} \rightarrow {}^1P_1 \\ \phantom{{}^3S_1} \rightarrow {}^3P_1 \end{array} \right| \begin{array}{l} I_f = 1 \\ 1 \\ 0 \\ 0 \\ 0 \\ 1 \end{array}$$

according to the widely used notation [17]. Among them, the amplitudes a , c , and d describe the parity conserving transitions, while the others violate parity. By writing the amplitudes

simply as

$$a_p \equiv \int \frac{p^2 dp}{(2\pi)^3} \int \frac{q^2 dq}{(2\pi)^3} \psi_0^{fin}(q; K^*) V_a^{proton}(p, q) \psi_0^{ini}(p) \quad (39)$$

for instance, one obtains

$$\Gamma_{\Lambda p \rightarrow pn} = \frac{M_N K^*}{2(2\pi)^2} \frac{1}{4} (|a_p|^2 + |b_p|^2 + 3|c_p|^2 + 3|d_p|^2 + 3|e_p|^2 + 3|f_p|^2) \quad (40)$$

$$\Gamma_{\Lambda n \rightarrow nn} = \frac{M_N K^*}{2(2\pi)^2} \frac{1}{4} (|a_n|^2 + |b_n|^2 + 3|f_n|^2) . \quad (41)$$

Note that the $I = 0$ states are allowed only for $\Lambda p \rightarrow pn$ while the $I = 1$ final states are allowed both for $\Lambda n \rightarrow nn$ and $\Lambda p \rightarrow pn$.

We employ simple wave functions for the initial and final states. We use the Gaussian with a short-range correlation function for the initial state,

$$\psi_{ini}(\vec{R}) = N_\psi g(\vec{R}) \exp \left\{ -\frac{1}{2B^2} \vec{R}^2 \right\} \quad (42)$$

where g represents the short range correlation,

$$g(\vec{R}) = 1 - C \exp \left[-\frac{R^2}{r_0^2} \right] . \quad (43)$$

For the final state we use the plane wave with the same short range correlation function,

$$\psi_{fin}(\vec{R}; \vec{K}^*) = g(\vec{R}) \exp \left\{ i\vec{K}^* \cdot \vec{R} \right\} . \quad (44)$$

We use the same $g(r)$ for the initial ΛN and the final NN only for simplicity. We choose the parameter B as $\sqrt{2} \times 1.3$ fm for the S-shell hypernuclei, which corresponds to the shell model wave function with the Gaussian parameter 1.3 fm for both the nucleon and Λ . For the short range correlation we choose $C = 0.5$ and $r_0 = 0.5$ fm = b in the present calculation. The strength C is chosen arbitrarily, while we find that the results are qualitatively the same for other values of C except for the proton asymmetry parameter a_1 (see section 6).

The one-pion exchange (OPE) amplitudes are also computed for the same wave functions.

We take the form factor ρ into account,

$$\mathcal{M} = \iiint d^3\vec{R}d^3\vec{r}_1d^3\vec{r}_2 \psi_{fin}^*(\vec{R})\rho(\vec{r}_1 - \frac{\vec{R}}{2})V_{\text{OPE}}(\vec{r}_1 - \vec{r}_2)\rho(\vec{r}_2 + \frac{\vec{R}}{2})\psi_{ini}(\vec{R}) , \quad (45)$$

where

$$\rho(\vec{r}) = \exp\left[-\frac{3}{2b^2}r^2\right] \quad (46)$$

represents the quark density in the baryon. Because $\Delta I = 1/2$ is assumed for the weak $\Lambda N\pi$ vertex, OPE amplitudes satisfy $a_n/a_p = b_n/b_p = f_n/f_p = \sqrt{2}$, while the $\Delta I = 3/2$ amplitudes give the ratio $-1/\sqrt{2}$. The weak $\Lambda N\pi$ coupling constant is adjusted to the free Λ decay rate.

The results for the two-body transition amplitudes are listed in Table 12. The numbers given under “ $\Delta I = 1/2(3/2)$ ” are the results with the pure $\Delta I = 1/2(3/2)$ transition potential. We find that the direct quark (DQ) amplitudes are in general comparable to the OPE ones, especially a_p, b_p, f_p and f_n for DQ are larger than those for OPE. Although a_n in the full DQ is small due to the cancellation of $\Delta I = 1/2$ and $\Delta I = 3/2$ amplitudes, it seems accidental because by changing the short-range correlation factor, the cancellation may disappear. While OPE contains only the $\Delta I = 1/2$ component, we find large $\Delta I = 3/2$ contributions for the $J = 0$ DQ transitions, a_p, b_p, a_n and b_n . The $\Delta I = 3/2$ contributions for f_p and f_n are small. The DQ amplitude d_p is zero because we neglect the tensor operator by truncating the p/m expansion at the order (p/m) . On the other hand, OPE has a large d_p which comes from the tensor part of the one-pion exchange interaction. It is enhanced due to the large momentum transfer.

Table 12: Calculated transition amplitudes in $10^{-10} \text{ MeV}^{-1/2}$.

		Direct Quark			OPE	
isospin	spin orbital	full	$\Delta I = 1/2$	$\Delta I = 3/2$		
a_p	$p\Lambda \rightarrow pn$	$^1S_0 \rightarrow ^1S_0$	-78.1	-23.4	-54.7	2.2
b_p		$\rightarrow ^3P_0$	-53.5	2.0	-55.5	-24.8
c_p		$^3S_1 \rightarrow ^3S_1$	-1.0	-1.0	0	2.2
d_p		$\rightarrow ^3D_1$	0	0	0	-86.8
e_p		$\rightarrow ^1P_1$	-23.2	-23.2	0	-43.0
f_p		$\rightarrow ^3P_1$	-55.4	-53.8	-1.5	20.2
a_n	$n\Lambda \rightarrow nn$	$^1S_0 \rightarrow ^1S_0$	5.5	-33.1	38.6	3.1
b_n		$\rightarrow ^3P_0$	42.2	2.9	39.3	-35.1
f_n		$^3S_1 \rightarrow ^3P_1$	-75.1	-76.2	1.0	28.6

6. Decays of S-shell hypernuclei

The spin averaged transition rates are decomposed as

$$\Gamma_{\Lambda p \rightarrow pn} = \frac{1}{4} (\Gamma_{p0} + 3\Gamma_{p1}) , \quad (47)$$

$$\Gamma_{\Lambda n \rightarrow nn} = \frac{1}{4} (\Gamma_{n0} + 3\Gamma_{n1}) , \quad (48)$$

where Γ_{NJ} is the transition rate for the two-body ΛN system with angular momentum J ,

$$\Gamma_{p0} = \frac{M_N K^*}{2(2\pi)^2} (|a_p|^2 + |b_p|^2) \quad (49)$$

$$\Gamma_{p1} = \frac{M_N K^*}{2(2\pi)^2} (|c_p|^2 + |d_p|^2 + |e_p|^2 + |f_p|^2) \quad (50)$$

$$\Gamma_{n0} = \frac{M_N K^*}{2(2\pi)^2} (|a_n|^2 + |b_n|^2) \quad (51)$$

$$\Gamma_{n1} = \frac{M_N K^*}{2(2\pi)^2} |f_n|^2 . \quad (52)$$

Our result for Γ_{NJ} are given in Table 13. We find that the $J = 0$ proton-induced transition rate, Γ_{p0} , is strongly enhanced due to the $\Delta I = 3/2$ transition. Compared with the OPE result, Γ_{p0} for DQ is much larger and in fact is dominant while OPE is dominated by the tensor transition included in Γ_{p1} . This dominance of Γ_{p1} in OPE makes the n - p ratio, R_{np} , small, where

$$R_{np} \equiv \frac{\Gamma_{\text{neutron induced}}}{\Gamma_{\text{proton induced}}} . \quad (53)$$

For the spin-average hypernuclei, ${}^5_{\Lambda}\text{He}$, this ratio is given by

$$R_{np} = \frac{\Gamma_{n0} + 3\Gamma_{n1}}{\Gamma_{p0} + 3\Gamma_{p1}} . \quad (54)$$

In DQ, Γ_{n1} is also large so that the spin averaged R_{np} is as large as 1. Thus we find that DQ and OPE predict qualitatively different values for $R_{np}({}^5_{\Lambda}\text{He})$, while the decay rates, $\Gamma({}^5_{\Lambda}\text{He})$, are roughly equal. The experimental data prefers DQ, which indicates a significant contribution of Γ_{n1} .

Recently, Schumacher proposed to check the $\Delta I = 1/2$ rule in the non-mesonic decays of the S-shell hypernuclei [19,20]. He calculated the ratios of Γ_{NJ} by using the following relations and the corresponding experimental data,

$$R_{np}({}^5_{\Lambda}\text{He}) = \frac{\Gamma_{n0} + 3\Gamma_{n1}}{\Gamma_{p0} + 3\Gamma_{p1}} \quad (55)$$

$$R_{np}({}^4_{\Lambda}\text{He}) = \frac{2\Gamma_{n0}}{\Gamma_{p0} + 3\Gamma_{p1}} \quad (56)$$

$$\frac{\Gamma({}^4_{\Lambda}\text{He})}{\Gamma({}^4_{\Lambda}\text{H})} = \frac{\Gamma_{p0} + 3\Gamma_{p1} + 2\Gamma_{n0}}{2\Gamma_{p0} + \Gamma_{n0} + 3\Gamma_{n1}} \quad (57)$$

where it is assumed that the Γ_{NJ} 's are common for ${}^5_{\Lambda}\text{He}$, ${}^4_{\Lambda}\text{He}$ and ${}^4_{\Lambda}\text{H}$. These equations determine three ratios of Γ_{NJ} 's. Using the experimental values of $\Gamma_{\Lambda p \rightarrow pn}$ and $\Gamma_{\Lambda n \rightarrow nn}$, we

Table 13: Decay rates of light hypernuclei. All the decay rates are in the unit of Γ_{free} . The experimental data for $\Gamma_{\Lambda p \rightarrow pn}$, $\Gamma_{\Lambda n \rightarrow nn}$, $\Gamma(^5_{\Lambda}\text{He})$ and $R_{np}(^5_{\Lambda}\text{He})$ are taken from ref. [18]. Those for $R_{np}(^4_{\Lambda}\text{He})$, $\Gamma_{n.m.}(^4_{\Lambda}\text{He})/\Gamma_{n.m.}(^4_{\Lambda}\text{H})$ and Γ_{n0}/Γ_{p0} are taken from ref. [19][20]. See the main text text for the “experimental” Γ_{NJ} ’s.

	Direct Quark		OPE	DQ \pm OPE		Exp
	Full	$\Delta I = \frac{1}{2}$		+	-	
Γ_{p0}	0.177	0.010	0.012	0.235	0.143	0 \sim 0.116
Γ_{p1}	0.071	0.067	0.193	0.260	0.269	0.074 \sim 0.187
Γ_{n0}	0.035	0.021	0.024	0.002	0.118	0.063 \sim 0.553
Γ_{n1}	0.111	0.114	0.016	0.042	0.212	0.049 \sim 0.196
$\Gamma_{\Lambda p \rightarrow pn}$	0.097	0.053	0.143	0.253	0.238	0.105 \pm 0.035
$\Gamma_{\Lambda n \rightarrow nn}$	0.092	0.091	0.018	0.032	0.189	0.100 \pm 0.055
$\Gamma(^5_{\Lambda}\text{He})$	0.378	0.295	0.333	0.573	0.854	0.41 \pm 0.14
$R_{np}(^5_{\Lambda}\text{He})$	0.94	1.70	0.12	0.12	0.79	0.93 \pm 0.55
$R_{np}(^4_{\Lambda}\text{He})$	0.18	0.20	0.08	0.004	0.24	0.18 \pm 0.12
$\frac{\Gamma_{n.m.}(^4_{\Lambda}\text{He})}{\Gamma_{n.m.}(^4_{\Lambda}\text{H})}$	0.63	0.66	6.58	1.69	1.14	1.65 \pm 0.77
Γ_{n0}/Γ_{p0}	0.20	2.00	2.00	0.01	0.854	-0.8 \pm 2.7
$a_1(^5_{\Lambda}\text{He})$	0.01	0.02	-0.19	0.20	-0.44	

evaluate the “experimental” values of Γ_{NJ} given in Table 13. The ratio Γ_{n0}/Γ_{p0} is especially sensitive to the $\Delta I = 3/2$ mixing, *i.e.*, it is 2 for the pure $\Delta I = 1/2$ transition, while it becomes 1/2 for the pure $\Delta I = 3/2$ transition. The second row from the bottom in Table 13 gives the ratio Γ_{n0}/Γ_{p0} . DQ gives a much smaller value than 2, which clearly demonstrates the contribution of $\Delta I = 3/2$. The present data, -0.8 ± 2.7 for the S-shell hypernuclei are not conclusive. One also sees that DQ mechanism can reproduce the n - p ratio for ${}^4_{\Lambda}\text{He}$, and the ratio $\Gamma({}^4_{\Lambda}\text{He})/\Gamma({}^4_{\Lambda}\text{H})$ fairly well.

When the hypernucleus is polarized, the angular distribution of the outgoing proton has an asymmetry. It is parameterized in terms of the asymmetry parameter a_1 as

$$W(\theta) = 1 + a_1(p) \mathcal{P}_{\Lambda} P_1(\cos \theta) . \quad (58)$$

where \mathcal{P}_{Λ} is the polarization of Λ and θ is the angle of the outgoing proton to the Λ polarization.

This parameter for ${}^5_{\Lambda}\text{He}$ is given by[11]

$$a_1({}^5_{\Lambda}\text{He}) = \frac{2\sqrt{3}(\sqrt{2}c_p + d_p)f_p}{a_p^2 + b_p^2 + 3(c_p^2 + d_p^2 + e_p^2 + f_p^2)} . \quad (59)$$

Recent experimental data indicate a large negative $a_1(p)$ for p-shell hypernuclei, $a_1(p) \leq -0.6$ [21]. Our result for $a_1({}^5_{\Lambda}\text{He})$ is very small because our d_p is zero and c_p is also small. But the result is rather sensitive to the choice of the short-range correlation, and therefore is not conclusive.

So far we have not considered the interference of the DQ and OPE amplitudes. As we have argued in section 3, the present formalism allows us to regard OPE independent from DQ and therefore to superpose these two amplitudes. Because the relation between the phenomenological $\Lambda N\pi$ vertex in OPE and the effective weak Hamiltonian $H_{eff}^{\Delta S=1}$ in DQ is not known, the relative phase of the two amplitudes cannot be determined. Thus we evaluate

DQ \pm OPE and the results are listed in Table 13. One finds that the difference between the two choices of the relative phase mostly appear in the neutron-induced decay rates. Γ_{nJ} 's are suppressed in (DQ + OPE) and thus the n - p ratio R_{np} becomes very small. In this sense, the experimental data prefer the (DQ - OPE) combination. (DQ - OPE) also predicts a large negative $a_1({}^5_{\Lambda}\text{He})$, which seems to agree with the experimental value for the p-shell hypernuclei. The ratio Γ_{n0}/Γ_{p0} tends to be small ($\ll 2$) for both (DQ \pm OPE) and again indicates a large $\Delta I = 3/2$ contribution. In both (DQ \pm OPE), we find that $\Gamma_{\Lambda p \rightarrow pn}$ is overestimated and therefore the total decay rate $\Gamma({}^5_{\Lambda}\text{He})$ is too large. This is again due to the large tensor component in $\Gamma_{p1}(\text{OPE})$. It seems important that OPE is calculated in the quark interaction point of view in order to make a reliable prediction for the DQ - OPE interference.

Recently Ramos and Bennhold studied contribution of the heavy meson exchanges such as K, ρ and η [22]. They indicate that such contributions are suppressed by the short range correlation and furthermore, they tend to cancel with each other. Recent studies of the 2π exchange mechanism indicate that the diagrams with ΣN and NN intermediate states cancel with each other and the net effect contributes only to the $J = 0$ amplitudes[23,24]. In all, the meson exchange contributions other than OPE seem to be small. Therefore one may describe the $\Lambda N \rightarrow NN$ transition well only by the DQ and OPE.

7. Discussions and Conclusion

Nonmesonic decays of hypernuclei provide us with a new type of the hadronic weak interaction. The large momentum transfer (due to the mass difference of Λ and N) makes the transition sensitive to the short distance quark structure of the two baryon system. Indeed, it is found that the contribution of the direct quark processes is as large as that of the con-

ventional one pion exchange weak interaction. Furthermore, we have found that the $J = 0$ transition amplitudes show a large $\Delta I = 3/2$ contribution and therefore that the $\Delta I = 1/2$ rule is significantly broken. This may be the first clear evidence for the $\Delta I = 3/2$ weak transition, that is expected in the standard theory of the weak interaction.

We have employed, in the present analysis, an effective weak Hamiltonian for quarks, which takes account of the one-loop perturbative QCD corrections. Then we have evaluated the transition amplitudes using the quark model wave functions of baryons to the first order in the weak interaction. The flavor/spin structure of the amplitudes reflects the SU(6) symmetry of the baryon wave functions, which have been verified in the low energy baryon spectrum and properties of the baryons.

We have derived an effective $\Lambda N \rightarrow NN$ transition potential, and applied it to the s-shell hypernuclear decays. It is found that the decay amplitudes show distinctive features when they are compared to the one-pion exchange. Especially, the ratio of the neutron-induced and the proton-induced decay rates is discriminative of these mechanisms. It is suggested that the ratios of the transition rates with various spin-isospin specification can be obtained from the experimental data for the s-shell hypernuclei and they are useful in testing different mechanisms of the transition. Further experimental studies are most desirable.

There are a number of remaining problems. The relation between the phenomenological $\Lambda \rightarrow N\pi$ transition Hamiltonian and the effective quark Hamiltonian is to be studied. It is favorable to apply the same quark Hamiltonian to the mesonic decay as well so that a unified view of the hypernuclear decay is obtained. The $\Delta I = 1/2$ enhancement mechanism for the mesonic decay is especially important in this regard. This line of study is underway and will be reported elsewhere[25].

For hypernuclei other than the s-shell systems, we need a realistic calculation combined with the nuclear structure analysis. We have provided the baryonic two-body transition potential that can be used in any hypernuclear structure calculations. Because of the nonlocal structure due to the quark exchange effects the transition potential is given in the momentum space, but the transformation into the coordinate space is straightforward.

We have not considered so far the second order process with a $\Sigma - N$ intermediate state induced by a strong pion (meson) and/or quark exchanges. The weak $\Sigma N \rightarrow NN$ decay can be also computed in the same direct quark mechanism. It is found that the mixing of ΣN does not change our main conclusions mentioned above, though its contribution is not negligible quantitatively. The results of this calculation will be published in a separate article[26].

Appendix A. Non-relativistic forms of $O_1 \sim O_6$

The Hamiltonian $H_{eff}^{\Delta S=1}$ is given by eq.(4):

$$H_{eff}^{\Delta S=1}(\mu \sim \mu_0) = -\frac{G_f}{\sqrt{2}} \sum_{r=1, r \neq 4}^6 K_r O_r \quad (60)$$

The operators, $O_2 \sim O_6$, contain the terms $(\bar{d}s)(\bar{s}s)$, which we omit because they do not contribute in the valence quark model. Then the Breit-Fermi expansion of $O_1 \sim O_6$ is given in terms of the operators $A1 \sim C11$ by

$$\begin{aligned} O_1 = & (A1 - C1) - (A2 - C2) - \frac{\delta}{2}(A3 - C3) \\ & - \frac{2\mu + \delta}{2}(A4 - C4) - \frac{\delta}{2}(A5 - C5) \\ & - \frac{2\mu + \delta}{2}(A6 - C6) - \frac{\delta}{2}(A7 - C7) - \frac{\delta}{2}(A8 - C8) \end{aligned} \quad (61)$$

$$\begin{aligned} O_2 = & (A1 + 2B1 + C1) - (A2 + 2B2 + C2) - \frac{\delta}{2}(A3 + 2B3 + C3) \\ & - \frac{2\mu + \delta}{2}(A4 + 2B4 + C4) - \frac{\delta}{2}(A5 + 2B5 + C5) \\ & - \frac{2\mu + \delta}{2}(A6 + 2B6 + C6) - \frac{\delta}{2}(A7 + 2B7 + C7) - \frac{\delta}{2}(A8 + 2B8 + C8) \end{aligned} \quad (62)$$

$$\begin{aligned} O_3 = & (2A1 - B1 + 2C1) - (2A2 - B2 + 2C2) - \frac{\delta}{2}(2A3 - B3 + 2C3) \\ & - \frac{2\mu + \delta}{2}(2A4 - B4 + 2C4) - \frac{\delta}{2}(2A5 - B5 + 2C5) \\ & - \frac{2\mu + \delta}{2}(2A6 - B6 + 2C6) - \frac{\delta}{2}(2A7 - B7 + 2C7) - \frac{\delta}{2}(2A8 - B8 + 2C8) \end{aligned} \quad (63)$$

$$\begin{aligned} O_5 = & (A1 + B1) + (A2 + B2) - \frac{\delta}{2}(A6 + B6) + \frac{\delta}{2}(A7 + B7) + \frac{\delta}{2}(A8 + B8) \\ & - \frac{\delta}{2}(A9 + B9) - \frac{2\mu + \delta}{2}(A10 + B10) + \frac{\delta}{2}(A11 + B11) \end{aligned} \quad (64)$$

$$\begin{aligned} O_6 = & -2 \left\{ (B1 + C1) - \frac{\delta}{4}(B3 + C3) + \frac{\delta}{4}(B4 + C4) + \frac{\delta}{4}(B5 + C5) \right. \\ & \left. + \frac{2\mu + \delta}{4}(B9 + C9) + \frac{\delta}{4}(B10 + C10) + \frac{\delta}{4}(B11 + C11) \right\} \end{aligned} \quad (65)$$

where

$$\mu \equiv \frac{m_s + m}{2m_s m} \text{ and } \delta \equiv \frac{m_s - m}{2m_s m}, \quad (66)$$

are given in terms of m , the mass of constituent u, d quarks, and m_s , the mass of constituent s quark. In the present calculation, we use $m = 313$ MeV and $m/m_s = 3/5$. Note that we have made the following Fierz transformation on O_6 so that the color part becomes unity.

$$O_6 = (\bar{d}_\alpha s_\beta)_{V-A} (\bar{u}_\beta u_\alpha + \bar{d}_\beta d_\alpha + \bar{s}_\beta s_\alpha)_{V+A} \quad (67)$$

$$= -2(\bar{d}_\alpha u_\alpha)_{S+P} (\bar{u}_\beta s_\beta)_{S-P} - 2(\bar{d}_\alpha d_\alpha)_{S+P} (\bar{d}_\beta s_\beta)_{S-P} \quad (68)$$

Appendix B. Flavor-spin part of $|\phi\phi\chi\rangle$

Table 14 gives the flavor-spin part of $|\phi\phi\chi\rangle$ for each Type. One sees that $|\phi\phi\chi\rangle$ is totally antisymmetric under the exchange $\{1,2,3\} \leftrightarrow \{4,5,6\}$. We choose either $s_z = 0$ or 1 so that $(s_i, \lambda^s, s_z, 0 | s_f, s_z)$ is not zero. These ‘‘Type’’s are referred to by the channels in Table 2.

Appendix C. Orbital matrix elements

The orbital part of the internal wave function of Λ and N is taken as

$$\phi(1, 2, 3)^{\text{orbital}} = N e^{-\frac{1}{2b^2}(\vec{r}_1 - \frac{\vec{r}_1 + \vec{r}_2 + \vec{r}_3}{3})^2} e^{-\frac{1}{2b^2}(\vec{r}_2 - \frac{\vec{r}_1 + \vec{r}_2 + \vec{r}_3}{3})^2} e^{-\frac{1}{2b^2}(\vec{r}_3 - \frac{\vec{r}_1 + \vec{r}_2 + \vec{r}_3}{3})^2} \quad (69)$$

where b denotes the size of the baryon. We choose $b = 0.5$ fm. It is convenient to use the Jacobi coordinates, defined in Table 15, in writing the orbital wave function of the two baryon system,

$$\phi(1, 2, 3)^{\text{orbital}} \phi(4, 5, 6)^{\text{orbital}} \chi \left(\frac{\vec{r}_1 + \vec{r}_2 + \vec{r}_3}{3} - \frac{\vec{r}_4 + \vec{r}_5 + \vec{r}_6}{3} \right). \quad (70)$$

Table 14: Flavor-Spin part of $|\phi\phi\chi\rangle$.

Ty.	Initial			Final		
	Orb.	Flavor	Spin	Orb.	Flavor	Spin
1	S	$\frac{1}{\sqrt{2}}(p\Lambda + \Lambda p)$	$\frac{1}{\sqrt{2}}(\uparrow\downarrow - \downarrow\uparrow)$	S	$\frac{1}{\sqrt{2}}(pn + np)$	$\frac{1}{\sqrt{2}}(\uparrow\downarrow - \downarrow\uparrow)$
2		+	-	P	+	+
3		-	+	S	-	+
4		-	+	P	-	-
5		-	$\uparrow\uparrow$	P	+	$\uparrow\uparrow$
A	P	+	$\uparrow\uparrow$	P	+	$\uparrow\uparrow$
B		+	$\frac{1}{\sqrt{2}}(\uparrow\downarrow + \downarrow\uparrow)$	S	+	$\frac{1}{\sqrt{2}}(\uparrow\downarrow - \downarrow\uparrow)$
C		+	$\uparrow\uparrow$	S	-	$\uparrow\uparrow$
F		-	$\frac{1}{\sqrt{2}}(\uparrow\downarrow - \downarrow\uparrow)$	S	-	$\frac{1}{\sqrt{2}}(\uparrow\downarrow + \downarrow\uparrow)$
G		-	-	P	-	-
6	S	$\frac{1}{\sqrt{2}}(n\Lambda + \Lambda n)$	$\frac{1}{\sqrt{2}}(\uparrow\downarrow - \downarrow\uparrow)$	S	nn	$\frac{1}{\sqrt{2}}(\uparrow\downarrow - \downarrow\uparrow)$
7		+	-	P	nn	+
8		-	$\uparrow\uparrow$	P	nn	$\uparrow\uparrow$
H	P	+	$\uparrow\uparrow$	P	nn	$\uparrow\uparrow$
I		+	$\frac{1}{\sqrt{2}}(\uparrow\downarrow + \downarrow\uparrow)$	S	nn	$\frac{1}{\sqrt{2}}(\uparrow\downarrow - \downarrow\uparrow)$

Table 15: Definition of the Jacobi coordinates and their conjugate momenta

$$\begin{aligned}
\vec{\xi}_{12} &= \vec{r}_1 - \vec{r}_2 & \leftrightarrow & \vec{p}_{12} = \frac{\vec{p}_1 - \vec{p}_2}{2} \\
\vec{\xi}_{12-3} &= \vec{r}_3 - \frac{\vec{r}_1 - \vec{r}_2}{2} & \leftrightarrow & \vec{p}_{12-3} = \frac{2}{3}\vec{p}_3 - \frac{\vec{p}_1 + \vec{p}_2}{3} \\
\vec{\xi}_{45} &= \vec{r}_4 - \vec{r}_5 & \leftrightarrow & \vec{p}_{45} = \frac{\vec{p}_4 - \vec{p}_5}{2} \\
\vec{\xi}_{45-6} &= \vec{r}_6 - \frac{\vec{r}_4 - \vec{r}_5}{2} & \leftrightarrow & \vec{p}_{45-6} = \frac{2}{3}\vec{p}_6 - \frac{\vec{p}_4 + \vec{p}_5}{3} \\
\vec{R} &= \frac{\vec{r}_1 + \vec{r}_2 + \vec{r}_3}{3} - \frac{\vec{r}_4 + \vec{r}_5 + \vec{r}_6}{3} & \leftrightarrow & \vec{P} = \frac{\vec{p}_1 + \vec{p}_2 + \vec{p}_3 - \vec{p}_4 - \vec{p}_5 - \vec{p}_6}{2} \\
\vec{R}_G &= \frac{\vec{r}_1 + \vec{r}_2 + \vec{r}_3 + \vec{r}_4 + \vec{r}_5 + \vec{r}_6}{6} & \leftrightarrow & \vec{P}_G = \vec{p}_1 + \vec{p}_2 + \vec{p}_3 + \vec{p}_4 + \vec{p}_5 + \vec{p}_6
\end{aligned}$$

The function $\phi(1, 2, 3)^{\text{orbital}}$ is written in terms of the Jacobi coordinates $\vec{\xi}_{12}$ and $\vec{\xi}_{12-3}$ as

$$\phi(1, 2, 3)^{\text{orbital}} = \left(\frac{1}{2\pi b^2}\right)^{\frac{3}{4}} \left(\frac{2}{3\pi b^2}\right)^{\frac{3}{4}} \exp\left\{-\frac{1}{4b^2}\xi_{12}^2\right\} \exp\left\{-\frac{1}{3b^2}\xi_{12-3}^2\right\} \quad (71)$$

or in the momentum space as

$$\phi(1, 2, 3)^{\text{orbital}} = (8\pi b^2)^{4/3} (6\pi b^2)^{3/4} \exp\left\{-b^2 p_{12}^2\right\} \exp\left\{-\frac{3}{4b^2} p_{12-3}^2\right\} . \quad (72)$$

Explicit forms of the orbital matrix elements

$$\langle \phi\phi(2\pi)^3 \delta(\vec{P}' - \vec{k}') | \mathcal{O}_{ij}(P_{36}) | \phi\phi(2\pi)^3 \delta(\vec{P} - \vec{k}) \rangle \quad (73)$$

are listed in Table 16 ~ Table 19. The matrix elements

$$\langle \phi\phi\chi(k', L_f) | \mathcal{O}_{ij} z(P_{36}) | \phi\phi\chi(k, L_i) \rangle \quad (74)$$

are given by the integration

$$\int d\hat{k}' \int d\hat{k} Y_{L_f}^{0*}(\hat{k}') \langle \phi\phi(2\pi)^3 \delta(\vec{P}' - \vec{k}') | \mathcal{O}_{ij}(P_{36}) | \phi\phi(2\pi)^3 \delta(\vec{P} - \vec{k}) \rangle Y_{L_i}^0(\hat{k}) . \quad (75)$$

Table 16: Orbital matrix elements.

$\mathcal{O}_{ij}(P_{36})$	$\langle \phi\phi(2\pi)^3\delta(\vec{P}' - \vec{k}') \mathcal{O}_{ij}(P_{36}) \phi\phi(2\pi)^3\delta(\vec{P} - \vec{k}) \rangle$
1_{12}	$\sqrt{2\pi}^3 \frac{1}{b^3} \frac{1}{k^2} \delta(k' - k)$
$1_{12} P_{36}$	$\frac{3\sqrt{6}}{4} \exp \left[-b^2 \left(\frac{5}{12} k^2 + \frac{1}{2} \vec{k} \cdot \vec{k}' + \frac{5}{12} k'^2 \right) \right]$
$1_{13} P_{36}$	$\frac{24\sqrt{33}}{121} \exp \left[-b^2 \frac{1}{33} (7k^2 + 12\vec{k} \cdot \vec{k}' + 13k'^2) \right]$
$1_{25} P_{36}$	$\frac{3\sqrt{3}}{8} \exp \left[-b^2 \frac{1}{6} (k^2 + k'^2) \right]$
$1_{35} P_{36}$	$\frac{24\sqrt{33}}{121} \exp \left[-b^2 \frac{1}{33} (13k^2 + 12\vec{k} \cdot \vec{k}' + 7k'^2) \right]$
1_{36}	$\exp \left[-b^2 \frac{1}{3} (k^2 + 2\vec{k} \cdot \vec{k}' + k'^2) \right]$
$1_{36} P_{36}$	$\exp \left[-b^2 \frac{1}{3} (k^2 + 2\vec{k} \cdot \vec{k}' + k'^2) \right]$

Table 17: Orbital matrix elements.

$\mathcal{O}_{ij}(P_{36})$	$\langle \phi\phi(2\pi)^3\delta(\vec{P}' - \vec{k}') \mathcal{O}_{ij}(P_{36}) \phi\phi(2\pi)^3\delta(\vec{P} - \vec{k}) \rangle$
\vec{q}_{12}	0
$\vec{q}_{12} P_{36}$	0
$\vec{q}_{13} P_{36}$	$\frac{1}{66} \left\{ -36\vec{k} + 12\vec{k}' \right\} \langle 1_{13} P_{36} \rangle$
$\vec{q}_{25} P_{36}$	$\frac{1}{66} \left\{ -33\vec{k} + 33\vec{k}' \right\} \langle 1_{25} P_{36} \rangle$
$\vec{q}_{35} P_{36}$	$\frac{1}{66} \left\{ -12\vec{k} + 36\vec{k}' \right\} \langle 1_{35} P_{36} \rangle$
\vec{q}_{36}	$\frac{1}{66} \left\{ -66\vec{k} + 66\vec{k}' \right\} \langle 1_{36} \rangle$
$\vec{q}_{36} P_{36}$	$\frac{1}{66} \left\{ +22\vec{k} + 22\vec{k}' \right\} \langle 1_{36} P_{36} \rangle$

Table 18: Orbital matrix elements.

$\mathcal{O}_{ij}(P_{36})$	$\langle \phi\phi(2\pi)^3\delta(\vec{P}' - \vec{k}') \mathcal{O}_{ij}(P_{36}) \phi\phi(2\pi)^3\delta(\vec{P} - \vec{k}) \rangle$
$(\vec{P}_1 - \vec{P}_2)$	0
$(\vec{P}_1 - \vec{P}_2) P_{36}$	0
$(\vec{P}_1 - \vec{P}_3) P_{36}$	$\frac{1}{66} \{ +36\vec{k} - 12\vec{k}' \} \langle 1_{13} P_{36} \rangle$
$(\vec{P}_2 - \vec{P}_5) P_{36}$	$\frac{1}{66} \{ +33\vec{k} + 33\vec{k}' \} \langle 1_{25} P_{36} \rangle$
$(\vec{P}_3 - \vec{P}_5) P_{36}$	$\frac{1}{66} \{ -12\vec{k} + 36\vec{k}' \} \langle 1_{35} P_{36} \rangle$
$(\vec{P}_3 - \vec{P}_6)$	$\frac{1}{66} \{ +22\vec{k} + 22\vec{k}' \} \langle 1_{36} \rangle$
$(\vec{P}_3 - \vec{P}_6) P_{36}$	$\frac{1}{66} \{ -66\vec{k} + 66\vec{k}' \} \langle 1_{36} P_{36} \rangle$

Table 19: Orbital matrix elements.

$\mathcal{O}_{ij}(P_{36})$	$\langle \phi\phi(2\pi)^3\delta(\vec{P}' - \vec{k}') \mathcal{O}_{ij}(P_{36}) \phi\phi(2\pi)^3\delta(\vec{P} - \vec{k}) \rangle$
$(\vec{P}_1 + \vec{P}_2)$	$\frac{1}{66} \{ +22\vec{k} + 22\vec{k}' \} \langle 1_{12} \rangle$
$(\vec{P}_1 + \vec{P}_2) P_{36}$	$\frac{1}{66} \{ +33\vec{k} - 33\vec{k}' \} \langle 1_{12} P_{36} \rangle$
$(\vec{P}_1 + \vec{P}_3) P_{36}$	$\frac{1}{66} \{ +12\vec{k} - 48\vec{k}' \} \langle 1_{13} P_{36} \rangle$
$(\vec{P}_2 + \vec{P}_5) P_{36}$	0
$(\vec{P}_3 + \vec{P}_5) P_{36}$	$\frac{1}{66} \{ -48\vec{k} + 12\vec{k}' \} \langle 1_{35} P_{36} \rangle$
$(\vec{P}_3 + \vec{P}_6)$	0
$(\vec{P}_3 + \vec{P}_6) P_{36}$	0

References

- [1] A.I. Vainshtein, V.I. Zakharov and M.A. Shifman, Sov. Phys. JETP, **45**(1977)670
- [2] F. J. Gillman and M. B. Wise, Phys. Rev. **D20**(1979)2382
- [3] E.A. Paschos, T. Schneider, and Y.L. Wu, Nucl. Phys. **B332**(1990)285
- [4] L.B. Okun, *Leptons and Quarks* (North Holland, The Netherlands, 1982)
- [5] C. Y. Cheung, D. P. Heddle and L. S. Kisslinger, Phys. Rev. **C27**(1983)335
- [6] K. Maltman and M. Shmatikov, Phys. Lett. **B311**(1994)1
- [7] M. Oka, T. Inoue and S. Takeuchi, Properties & Interactions of Hyperons,
Proceedings of the U.S.-Japan Seminar ed. by B. F. Gibson, P. D. Barnes and K. Nakai
(World Scientific, 1994)
- [8] T. Inoue, S. Takeuchi and M. Oka, Nucl. Phys. **A577**(1994)281c
- [9] K. Takeuch, H. Takaki and H. Bando, Prog. Theor. Phys. **73**(1985)841
- [10] A. Ramos, E. van Meijgaard, C. Bennhold, and B. K. Jennings,
Nucl. Phys. **A544**(1992)703
- [11] H. Bando, T. Motoba and J. Zofka, Int. Jour. Mod. Phys. **A5**(1990)4021
- [12] J. Cohen, Prog. in Part. and Nucl. Phys. **25**(1990)139
- [13] W.A. Bardeen, A.J. Buras and J.M. Gerard Phys. Lett. **B192**(1987)138
- [14] T. Morozumi, C.S. Lim, A.I. Sanda, Phys. Rev. Lett. **65**(1990)404
- [15] M. Takizawa, T. Inoue, and M. Oka, INS-Rep.-1089
to be published in Prog. Theor. Phys. Suppl.
- [16] M. Oka and K. Yazaki, Phys. Lett. **B90**(1980)41
- [17] M.M. Block and R.H. Dalitz, Phys. Rev. Lett. **11**(1963)96

- [18] J.J. Szymanski *et al.* Phys. Rev. **C43**(1991)849
- [19] R.A. Schumacher, Nucl. Phys. **A547**(1992)143c
- [20] R.A. Schumacher, Properties & Interactions of Hyperons,
Proceedings of the U.S.-Japan Seminar ed. by B. F. Gibson, P. D. Barnes and K. Nakai
(World Scientific, 1994)
- [21] T. Kishimoto, Properties & Interactions of Hyperons,
Proceedings of the U.S.-Japan Seminar ed. by B. F. Gibson, P. D. Barnes and K. Nakai
(World Scientific, 1994)
- [22] A. Ramos and C. Bennhold, Nucl. Phys. **A577**(1994)287c
- [23] M. Shmatikov, Preprint IAE-5708/2 M. 1994
- [24] K. Itonaga, T. Ueda and T. Motoba, Nucl. Phys. **A577**(1994)301c
- [25] T. Inoue, M. Takizawa and M. Oka, to be published
- [26] T. Inoue, S. Takeuchi and M. Oka, to be published